

FRACTURE MECHANISMS IN B2 NiTi SHAPE MEMORY ALLOYS

Nancy Yang¹, Ken Gall², Huseyin Sehitoglu³, and Yuriy Chumlyakov⁴

¹Materials & Engineering Sciences Center, Sandia National Laboratories,
Livermore, CA, 94550 USA

²Department of Mechanical Engineering, University of Colorado, Boulder, CO, 80309 USA

³Department of Mechanical and Industrial Engineering, University of Illinois at Urbana-
Champaign, Urbana, IL, 61801 USA

⁴Tomsk University, 634050 Tomsk, Russia

ABSTRACT

The fracture mechanisms in single crystal Ti-50.8at%Ni shape memory alloys containing Ti_3Ni_4 precipitates are studied using the scanning electron microscope (SEM). Aged materials with three different precipitate sizes (50 nm, 150 nm, and 400 nm), which have interfaces ranging from semi-coherent to incoherent, are considered. The primary mechanisms of material fracture identified in the single crystal NiTi are: (1) Nucleation, growth, and coalescence of voids from the Ti_3Ni_4 precipitates and (2) Cleavage fracture on $\{100\}$ crystallographic planes. Cleavage fracture and ductile tearing are found to act in conjunction, and the relative dominance of one over the other depends on the local precipitate size. When the Ti_3Ni_4 precipitates are small and coherent they facilitate mechanism 2. As the Ti_3Ni_4 precipitate size increases to about 400 nm, the overall fracture is dominated by failure mechanism 1, and the cleavage markings become diffuse.

KEYWORDS

NiTi, Single Crystals, Cleavage Fracture, Ductile Tearing.

INTRODUCTION

As evident in a recent review on shape memory alloys [1], the general thermo-mechanical response of NiTi is well characterized for various testing conditions. However, the utilization of NiTi shape memory alloys in long life components requires a thorough understanding of the dominant mechanisms controlling their fatigue and fracture. Under cyclic loading conditions, the failure of NiTi shape memory alloys in service can be caused by either an inability of the alloy to provide the required material response (recoverable displacement or force) or the fracture of the material. Minimal work [2] has been performed on the resistance of NiTi alloys

to fatigue crack growth and fracture. Understanding the fatigue crack growth and fracture behavior of NiTi alloys is imperative for applications where the alloys are subjected to a combination of low cycle fatigue (active use of the transformation) and high cycle fatigue (inactive structural support) conditions. Such loading sequences facilitate the formation of microcracks that can lead to premature fracture of the shape memory alloy component. The present study will consider the fracture mechanisms in single crystal Ti-50.8at%Ni with three different Ti_3Ni_4 precipitate sizes.

MATERIALS AND METHODS

Ti-50.8at%Ni single crystal specimens were grown from a single material batch using the modified Bridgeman technique in an inert gas atmosphere in the temperature range 1773 K – 1893 K. Following growth, the crystals were homogenized at 1273 K for 24 hours in a vacuum furnace and quenched into ambient temperature water, leaving them in the solutionized state. The solutionized single crystal NiTi materials were given subsequent aging treatments of 1.5 hr @ 723 K, 1.0 hr @ 773 K, and 1.5 hr @ 823 K which resulted in Ti_3Ni_4 precipitates with sizes of 50 nm, 150 nm, and 400 nm, respectively.

Mechanical tests were conducted at room temperature ($T = 298$ K) in laboratory air conditions. Monotonic and cyclic tests (total strain range of 3%, $R = 0$) were conducted until complete fracture of the specimens. Monotonic tests were conducted on samples aged 1.0 hr @ 773 K with a [100] loading axis orientation. Cyclic tests on the crystals with a [148] loading axis orientation were conducted on materials aged 1.5 hr @ 723 K and 1.5 hr @ 823 K. Material regions on the fracture surface that failed through overload during the monotonic and cyclic tests were examined with the Scanning Electron Microscope (SEM).

FRACTOGRAPHY

The overall fracture surfaces of the three fractured NiTi samples are shown in Figure 1. The crystallographic orientations of the tensile axes (the direction out of the paper) are indicated to the right of the images and the heat treatments are indicated above the appropriate fracture surface image. In general, as the Ti_3Ni_4 precipitate size increases, and the precipitates lose coherency, the fracture surface demonstrates a rougher appearance, indicating a transition to more ductile local fracture mechanisms. In single crystals, the overall orientation of the fracture surface with respect to the applied tensile axis can give insight into the operative fracture mechanisms. The only fracture surface in Figure 1 perpendicular to the applied tensile axis is the sample loaded along the [100] direction. The samples oriented along [148] demonstrated fracture surfaces with a normal misoriented with respect to the tensile axis. Since the specimens loaded along the [100] direction demonstrated fracture surfaces oriented 90 degrees from the tensile axis, it appears that the {100} planes serve as cleavage planes in NiTi. Previous studies on B2 intermetallics have found that both the {100} and {110} planes can act as cleavage planes [3].

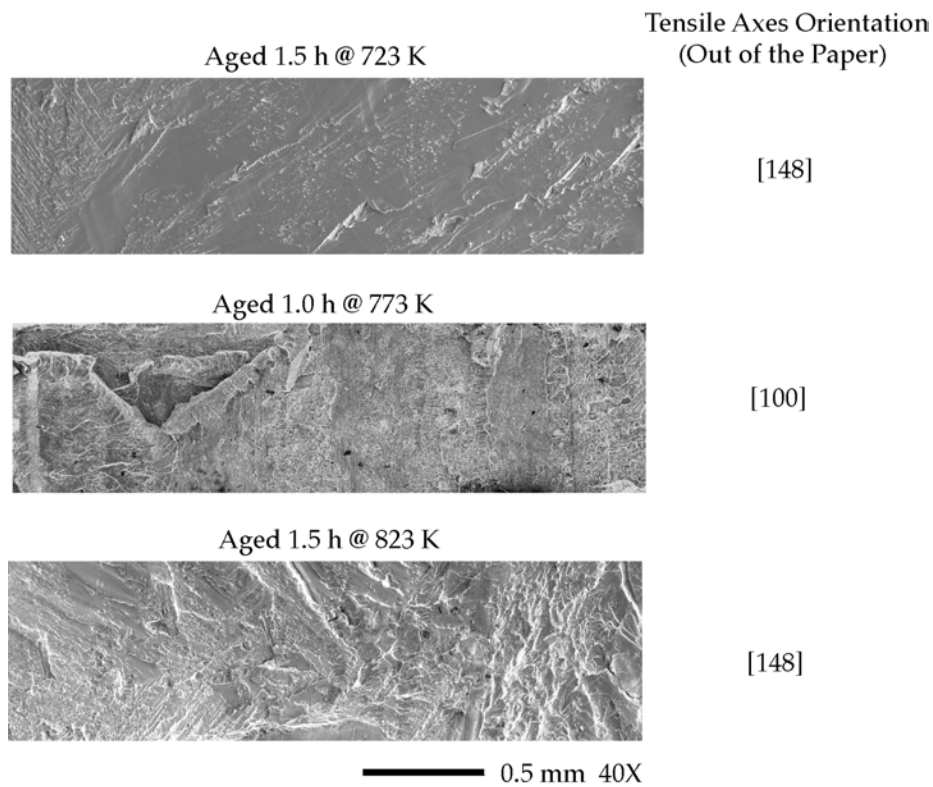


Figure 1: SEM images of the overall appearance of the fracture surfaces.

In order to confirm the above macroscopic observations, higher magnification images of the fracture surface are required. In Figure 2, a SEM image of from fracture surface of the specimen loaded along the [100] orientation demonstrates markings typical of cleavage fracture.

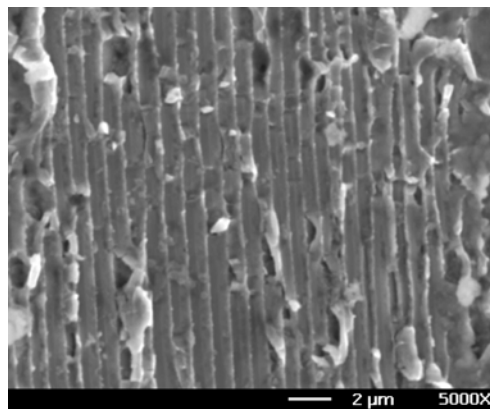


Figure 2: SEM image of the fracture surface of the [100] crystal aged 1.0 hr @ 773 K.

As such, it is confirmed that the NiTi crystals undergo local material cleavage in some regions of the specimen. The markings in Figure 2 have facets on the $\{100\}$ planes, with crack growth along the $[0\bar{1}1]$ direction and a crack line along the $[011]$ direction. We note that the observed cleavage planes have a correspondence to the highly symmetric B2 parent phase rather than any relation to the habit planes of the low symmetry Type II B19' martensite plates, $(-0.88, 0.21, 0.40)$. Such an observation circumvents any relation between the propagation of overload cracks

and the orientation of the martensite plates; however, it is still possible that the plates nucleate fracture and this is a topic of future research.

Figure 3 shows high resolution images from the [148] crystals, comparing the cleavage markings for samples aged (a) 1.5 hr @ 723 K versus (b) 1.5 hr @ 823 K. The orientations of the markings are the same for samples aged under the two different conditions (they are mirror

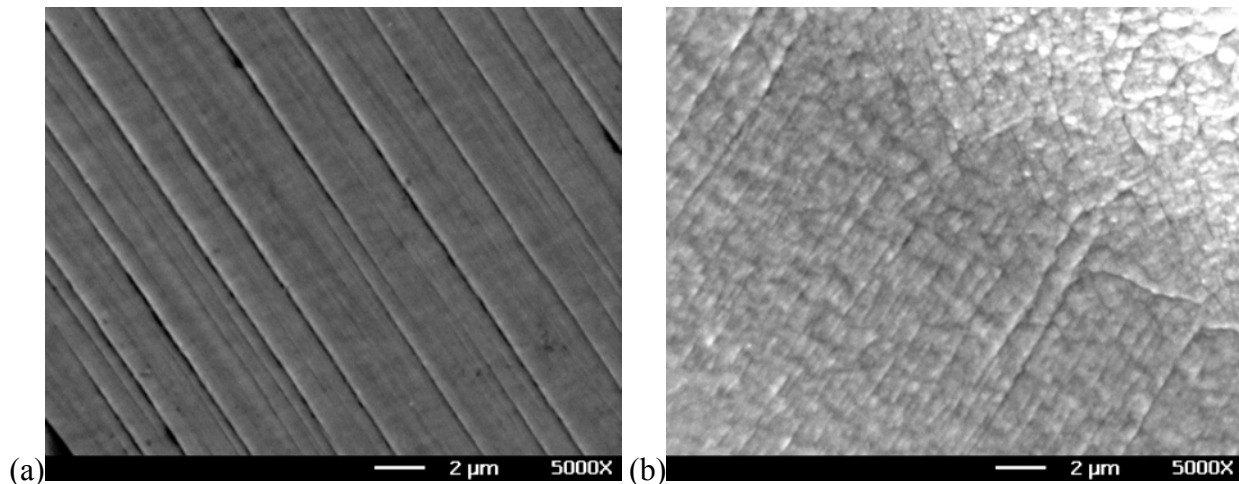


Figure 3: SEM image of cleavage patterns on the fracture surfaces of the [148] crystal aged (a) aged 1.5 hr @ 723 K or (b) 1.5 hr @ 823 K.

images of each other due to the opposite choice of fracture sample halves). However, the cleavage markings in Figure 3b are wavy, and have considerable surface roughness compared to the distinct markings in Figures 3a. In general, a rougher appearance to the fracture surface implies an increased amount of local plastic flow during fracture. In other words, even though the crystallographic aspects of the cleavage fracture are still evident in the samples with the larger Ti_3Ni_4 precipitates, the cleavage occurs with more local distortion than in samples with relatively smaller Ti_3Ni_4 precipitates.

We assert that the increased distortion during cleavage in the samples with the larger precipitates is caused by the local composition changes during the aging process. As Ti_3Ni_4 precipitates coarsen, the local Ni concentration is decreased since the precipitates are Ni rich compared to the matrix. The observations in Figure 3 clearly imply that supersaturated Ni-rich NiTi is inherently more brittle than equiatomic NiTi. Figure 4 lends further support to the above hypothesis on the different fracture mechanisms in the NiTi alloys given the two different aging treatments. The image in Figure 4a was taken in a region of the sample where the Ti_3Ni_4 precipitates are much larger than the average size for the 1.5 hr @ 723 K treatment. Conversely, the visible precipitates in the image in Figure 4b are more typical of the precipitates found in the samples aged 1.5 hr @ 823 K. In the NiTi aged 1.5 hr @ 723 K the cleavage path generally cuts straight through the regions with the large precipitates, leaving negligible voids surrounding them. However, in the alloy aged 1.5 hr @ 823 K the cleavage path is hardly recognizable, except for faint lines, and significant dimples surround the larger precipitates. We note that precipitates much smaller than the ones visible in the holes in figure 4a may exist in the surrounding material. The local deformation characteristics near these smaller precipitates (50-100 nm), coupled with the high Ni concentration of the surrounding matrix, are responsible for the cleavage fracture in Figure 4a versus the ductile fracture in Figure 4b. Such observations are

consistent with previous findings on aluminum alloys where peak aged alloys have a lower toughness compared to overaged alloys [4]. In the aluminum alloys, it has been demonstrated that the finer peak aged precipitates facilitate strong localization and rapid crack extension, rather than crack tip blunting through extensive plasticity [4]. We note that the above observations were typical for the samples given the distinctly different aging treatments.

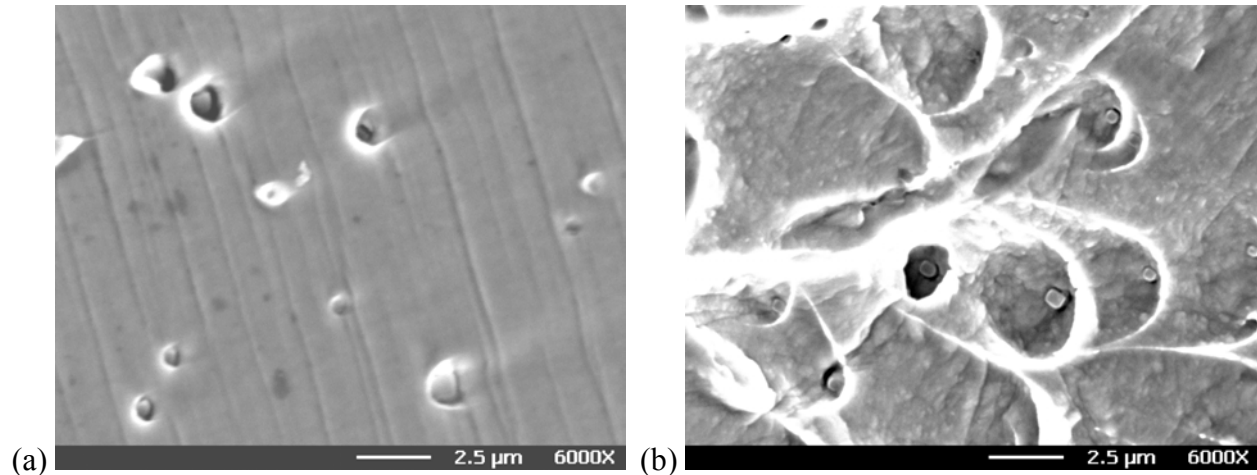


Figure 4: SEM image of dimpled fracture from relatively large second phase Ti_3Ni_4 precipitates on the fracture surfaces of the [148] crystal aged (a) aged 1.5 hr @ 723 K or (b) 1.5 hr @ 823 K.

RAMAFICATIONS AND CONCLUSIONS

The fracture of aged single crystal Ti-50.8at%Ni shape memory alloys containing Ti_3Ni_4 precipitates is controlled by cleavage on the $\{100\}$ planes coupled with void nucleation, growth, and coalescence from the second phase particles. The two mechanisms of material failure act in conjunction with one another and the dominance of one over the other depends on the relative size of the Ti_3Ni_4 precipitates and the Ni concentration of the matrix. As the average precipitate size increases, the frequency of large dimples near second phase particles also increases.

In materials containing semi-coherent Ti_3Ni_4 precipitates (50 –150 nm), cleavage fracture is distinct and markings appear consistent with markings from traditional intermetallic materials. However, when the Ti_3Ni_4 precipitates are larger (400 nm) and incoherent, the markings are wavy and the cleavage fracture planes become locally distorted. Based on the above observation, it is asserted that the Ni-rich supersaturated NiTi matrix surrounding the precipitates is more brittle than a pure NiTi matrix.

Most drawn wire and bar stock NiTi has a strong fiber texture of the $\{111\}$ type along the drawing direction. Since the martensitic transformation is triggered at a lower applied tensile stress level as the crystal orientation approaches the [111]-[110] symmetry boundary, such textured polycrystalline alloys are “favorably” oriented for the transformation under tension. Moreover, alloys with such a favorable transformation texture do not have $\{100\}$ cleavage planes favorably oriented for fracture. Consequently, the well-documented high tensile ductility (along the drawing direction) of bar and wire stock polycrystalline NiTi alloys is partially attributed to the favorable orientation of the transformation coupled with the unfavorable orientation of $\{100\}$ cleavage planes.

ACKNOWLEDGMENTS

The research of K. Gall and H. Sehitoglu is supported by a grant from the Department of Energy, Basic Energy Sciences Division, Germantown, Maryland, DOE DEFG02-93ER14393. The research of N. Yang is funded by the Department of Energy. The work of Y. Chumlyakov is supported by grants from the Russian Fund for Basic Researches, grant # 02-95-00350, MOPO (MGU, Moscow) and from fund 99-03-32579a.

REFERENCES

- [1] Otsuka, K and Wayman, C. M. (1998) *Shape Memory Materials*, Cambridge University Press, New York, NY.
- [2] Melton, K. N. and Mercier, O. (1979) *Acta. Metall.*, 27, 137.
- [3] Chang, K.-M., Darolia, R., and Lipsitt, H. A. (1992) *Acta. Metall. Mater.*, 40, 2727.
- [4] Hahn, G. T. and Rosenfield, A. R. (1975) *Metall. Trans.*, 6A, 653.
- [5] Bhattacharya, K. and Kohn, R. V. (1996) *Acta Mater.*, 44, 529.
- [6] Shu, Y. C. and Bhattacharya, K. (1998) *Acta Mater.*, 46, 5457.
- [7] Gall, K., Sehitoglu, H., Chumlyakov, Y. I., and Kireeva, I. V. (1999) *Acta Mater.*, 47, 1203.